The Astrophysical Journal, 645:1283–1296, 2006 July 10

THE *SPITZER* c2d SURVEY OF WEAK-LINE T TAURI STARS. I. INITIAL RESULTS

Deborah L. Padgett,[1] Lucas Cieza,[2] Karl R. Stapelfeldt,[3] Neal J. Evans, II,[2] David Koerner,[4] Anneila Sargent,[5] Misato Fukagawa,[1] Ewine F. van Dishoeck,[6] Jean-Charles Augereau,[6] Lori Allen,[7] Geoff Blake,[5] Tim Brooke,[5] Nicholas Chapman,[8] Paul Harvey,[2] Alicia Porras,[7] Shih-Ping Lai,[8] Lee Mundy,[8] Philip C. Myers,[7] William Spiesman,[2] and Zahed Wahhaj[4]

Received 2006 February 2; accepted 2006 March 13

ABSTRACT

Using the *Spitzer Space Telescope*, we have observed 90 weak-line and classical T Tauri stars in the vicinity of the Ophiuchus, Lupus, Chamaeleon, and Taurus star-forming regions as part of the Cores to Disks (c2d) *Spitzer* Legacy project. In addition to the *Spitzer* data, we have obtained contemporaneous optical photometry to assist in constructing spectral energy distributions. These objects were specifically chosen as solar-type young stars with low levels of Hα emission, strong X-ray emission, and lithium absorption, i.e., weak-line T Tauri stars, most of which were undetected in the mid- to far-IR by the *IRAS* survey. Weak-line T Tauri stars are potentially extremely important objects in determining the timescale over which disk evolution may take place. Our objective is to determine whether these young stars are diskless or have remnant disks that are below the detection threshold of previous infrared missions. We find that only 5/83 weak-line T Tauri stars have detectable excess emission between 3.6 and 70 μm, which would indicate the presence of dust from the inner few tenths of an AU out to the planet-forming regions a few tens of AU from the star. Of these sources, two have small excesses at 24 μm consistent with optically thin disks; the others have optically thick disks already detected by previous IR surveys. All of the seven classical T Tauri stars show excess emission at 24 and 70 μm although their properties vary at shorter wavelengths. Our initial results show that disks are rare among young stars selected for their weak Hα emission.

Subject headings: infrared: stars — planetary systems: protoplanetary disks — stars: pre–main-sequence

Online material: color figures

1. INTRODUCTION

T Tauri stars (Joy 1945) have long been known as solar-mass pre–main-sequence (PMS) stars. Sprinkled throughout molecular cloud complexes, or gathered in dense clusters, they have traditionally been identified by their unusual optical spectra, which include bright emission lines of Hα and other permitted and forbidden atomic transitions. However, with the advent of X-ray molecular cloud surveys, another class of solar-type young star has been identified from their high X-ray luminosity. Unlike the spectroscopically identified "classical" T Tauri stars (CTTSs), these objects lack Hα emission in excess of 10 Å in equivalent width (EW) and are thus known as "weak-line" T Tauri stars (WTTSs; Herbig & Bell 1988). Confirmation that X-ray–identified WTTSs are young stars requires high-resolution optical spectra that show a solar-type spectrum with a Li I λ6707 absorption line EW stronger than that of a Pleiades star of the same spectral type (Covino et al. 1997). The presence of a strong lithium absorption indicates stellar youth among stars with deeply convecting photospheres since lithium is easily destroyed at high temperatures. In practice, using the Li I EW to select young stars is a difficult task, since the strength of the lithium line may depend on the rotational history of the star and spot coverage (Mendes et al. 1999). In addition, spectral classes earlier than G5 may retain strong lithium lines throughout their main-sequence lifetimes (Spite et al. 1996). Thus, current lists of WTTSs are probably contaminated to some degree by young main-sequence stars that are closer than the cloud but too faint for accurate parallax measurements (Alcala et al. 1998).

The current paradigm of planet formation is still based on the venerable *IRAS* (Strom et al. 1989) and millimeter continuum surveys (Beckwith et al. 1990) of the late 1980s that found mid- to far-infrared and/or millimeter excess emission around about half of solar-type stars in nearby clouds. This picture of disk evolution starts with Class 0–I sources, which are extremely faint shortward of 25 μm, proceeds through Class I with a rising IR spectral energy distribution (SED), continues to Class II, which has a flat or falling SED with strong IR excesses above the photosphere, and ends at Class III, where the excess emission indicates a tenuous, optically thin disk (Adams et al. 1987; André & Montmerle 1994). In practice, *IRAS* and the *Infrared Space Observatory* (*ISO*) were not sensitive enough to detect optically thin disks in the mid-IR at the distance of nearby star formation regions; however, the *Spitzer Space Telescope* does have this capability. Almost as soon as the first WTTSs were identified, they were presumed to be the Class III "missing link" of the planet formation paradigm since "post"–T Tauri stars had proved elusive. Initial ground-based near-infrared (NIR) and mid-infrared (MIR) studies showed that inner disks were very rare among the

[1] *Spitzer* Science Center, California Institute of Technology, Mail Code 220-6, Pasadena, CA 91125; dlp@ipac.caltech.edu.
[2] Astronomy Department, University of Texas, 1 University Station C1400, Austin, TX 78712.
[3] Jet Propulsion Laboratory, MS 183-900, 4800 Oak Grove Drive, Pasadena, CA 91109.
[4] Department of Physics and Astronomy, Northern Arizona University, Box 6010, Flagstaff, AZ 86011.
[5] Astronomy Option, California Institute of Technology, MS 105-24, Pasadena, CA 91125.
[6] Leiden Observatory, Postbus 9513, 2300 R.A. Leiden, Netherlands.
[7] Smithsonian Astrophysical Observatory, Harvard-Smithsonian Center for Astrophysics, 60 Garden Street, MS 42, Cambridge, MA 02138.
[8] Astronomy Department, University of Maryland, College Park, MD 20742.

WTTS population (Skrutskie et al. 1990). More recent *JHKL* studies of several young clusters indicated that inner disks disappear in 5–6 Myr (Haisch et al. 2001). On the other hand, a *JHKL* study of the ≈10 Myr η Cha cluster found a rather high disk fraction among its few known members (Lyo et al. 2003), although a smaller percentage of disks was found by Haisch et al. (2005). Both *IRAS* and millimeter surveys indicate that optically thick outer disks are rare among WTTSs (Strom et al. 1989; Osterloh & Beckwith 1995). However, a sensitive study of tenuous material in the terrestrial-planet–forming zone of WTTSs has awaited the power of the *Spitzer Space Telescope*. *Spitzer* has over 1000 times the sensitivity at 24 μm of *IRAS*, with similar improvements in its other imaging bands (Werner et al. 2004). Only *Spitzer* can distinguish between transitional disks (optically thick with inner holes), optically thin remnant disks with low disk luminosity L_d ($L_d/L_* \ll 1$, like the debris disks found around older stars), and completely diskless "naked" T Tauri stars.

Study of circumstellar material around WTTSs promises to answer some significant questions about planet formation around low-mass stars. The first is whether some young stars are born "diskless," that is, some stars at the age of 1–3 Myr do not retain remnant circumstellar material and did not possess substantial disks long enough for plausible planet formation. Typical "core accretion" models of giant planet formation require a minimum of 5 million years to make a jupiter, most of which is spent in the coagulation of dust and accretion of planetesimals (Weidenschilling 2000), although accretion times continue to drop in the most recent models (Goldreich et al. 2004a, 2004b) and the alternative "disk instability" model can produce giant planets on a very short timescale (Boss 2001). A low detection frequency of any infrared excess among WTTSs would provide evidence for diskless young stars. In addition, this study will address the dispersion in disk properties among coeval stars in the same environment. These differences could possibly be related to the early formation of planets in the stars where the disks have inner holes or have disappeared entirely. Such a hypothesis is potentially testable with future high-resolution astrometric studies of young stars with and without disks to see if the presence of giant planets is related to the state of disk evolution.

Several *Spitzer* surveys to assess the detection frequency of excess in young stars either are in progress or have been published recently. The entire range of *Spitzer* instrumentation is utilized by these studies, including the 3.6–8.0 μm Infrared Array Camera (IRAC), the 24, 70, and 160 μm Multiband Imaging Photometer (MIPS), and the 5–40 μm Infrared Spectrograph (IRS). There are several investigations of excess among very young stars in individual star-forming regions (e.g., Reach et al. 2004; Muzerolle et al. 2004; Padgett et al. 2004; Young et al. 2005; Hartmann et al. 2005a). These studies investigate known young star populations including WTTSs, CTTSs, and Class I sources. Among older PMS associations, Chen et al. (2005) report on an MIPS 24 and 70 μm survey of 40 F- and G-type stars in the Sco-Cen OB association with an age of 5–20 Myr (Chen et al. 2005). The Megeath et al. (2005) IRAC study of η Cha covers the stellar population of this 8–10 Myr association. A similar investigation with MIPS of the TW Hydrae group is detailed in Low et al. (2005). Young main-sequence clusters such as M47 (Gorlova et al. 2004) and the Pleiades (Stauffer et al. 2005) have been studied using MIPS. For older Population I stars, Beichman et al. (2005) and Bryden et al. (2006) present results from a very sensitive 24 μm, 70 μm (MIPS), and *Spitzer* IRS survey of generally old, but very bright, solar neighborhood stars. Due to the brightness of their targets and selection for low IR backgrounds, this program has much higher sensitivity at 70 μm than the other studies, enabling detection of very tenuous cold disks invisible to other surveys. Two surveys that span a wide range of stellar ages are Rieke et al. (2005) and the "Formation and Evolution of Planetary Systems" *Spitzer* Legacy project or FEPS (Meyer et al. 2004). For stars more massive than the Sun, Rieke et al. (2005) survey A-type stars of 5–850 Myr at 24 μm with MIPS. FEPS is examining stars with ages ranging from 3 Myr to 3 Gyr, divided into bins for stars of roughly equivalent ages (Meyer et al. 2004). The large age span for FEPS means that their sample has a large number of faint young stars at distances over 100 pc and a smaller number of bright nearby old stars for which 70 μm sensitivities are good. Although their youngest age group includes solar-type stars of similar age to the current WTTS sample, the FEPS young stars are located more than 6° from nearby clouds (Silverstone et al. 2006). In contrast to these surveys, our 0.5–70 μm survey focuses only on WTTSs in and adjacent to several star-forming clouds within 200 pc.

The current work is the first of three papers that will discuss disks around WTTSs in the c2d *Spitzer* data. Paper I discusses initial results for 90 stars specifically targeted for photometric mode observations with IRAC and MIPS. Most of these sources fall outside of high-extinction regions but within 6° of cloud centers. Paper II (L. Cieza et al. 2006, in preparation) will present SEDs for WTTSs that fall within the large c2d cloud maps of Perseus, Ophiuchus, Lupus, Chamaeleon, and Serpens. Paper III (Z. Wahadj et al. 2006, in preparation) will present the remainder of the individually targeted WTTSs, provide upper limits for the 70 μm nondetections, and interpret the entire sample in terms of debris disk models.

2. OBSERVATIONS

2.1. *Target Selection*

The c2d WTTS survey source selection focuses on targets associated with nearby molecular clouds being mapped by large *Spitzer* mapping surveys. Only for nearby targets ($d < 200$ pc) can *Spitzer* achieve the needed sensitivity to optically thin dust in the planet formation region around a zero-age main-sequence (ZAMS) low-mass star, over a statistically meaningful sample, and in the 50 hr of observing time allocated for this study. Molecular cloud association is crucial for establishing a star's youth: over 10 Myr, the measured proper-motion dispersion for young stars at $d \sim 140$ pc can carry them 6° of projected separation away from their formation region (Hartmann et al. 1991). We therefore required that our WTTS targets lie within this radius from their associated cloud. About $\frac{1}{3}$ of the sample lies within the clouds, $\frac{1}{3}$ are adjacent to the clouds, and $\frac{1}{3}$ are 3°–6° from the clouds. Selecting WTTSs associated with clouds being mapped by *Spitzer* also allows an eventual comparison between the WTTS disk properties and those of the younger cloud population; both presumably formed under similar conditions. In the end, rich but distant regions of low-mass star formation (Orion, Serpens, Perseus) were rejected for study in favor of those in the distance range 120–160 pc: Taurus, Lupus, Ophuichus, and Chamaeleon. The latter three are being mapped by the c2d project (Evans et al. 2003), and a separate large *Spitzer* survey of Taurus is also being carried out (Güdel et al. 2006).

The *ROSAT* mission of 1990–1998 identified a sizable population of X-ray active stars in and around the four nearby clouds targeted for this WTTS study (Wichmann et al. 1996, 1997). X-ray activity is a signature of stellar youth and is correlated with

TABLE 1

Spitzer Observations

ID	R.A. (deg)	Decl. (deg)	IRAC Observation Date	MIPS Observation Date	Notes[a]
NTTS 032641+2420	52.40987	24.51053	2004 Aug 16	2004 Sep 19	
RX J0405.3+2009	61.33163	20.15711	2004 Sep 07	2004 Sep 22	
NTTS 040234+2143	61.37862	21.85294	2005 Feb 22	2004 Sep 25	
RX J0409.2+1716	62.32083	17.26892	2004 Sep 07	2004 Sep 25	
RX J0409.8+2446	62.46304	24.77253	2004 Sep 08	2004 Sep 25	
RX J0412.8+1937	63.21100	19.61614	2004 Sep 07	2004 Sep 25	IRAC C2 with RX J0405.3+2009
NTTS 041559+1716	64.71542	17.38792	2004 Sep 07	2004 Sep 25	
RX J0420.3+3123	65.10050	31.38992	2004 Sep 07	2004 Sep 19	
RX J0424.8+2643a	66.20433	26.71956	2004 Sep 07	2004 Sep 25	
RX J0432.8+1735	68.22179	17.59269	2004 Sep 07	2004 Sep 25	
RX J0437.4+1851a	69.36192	18.85744	2004 Sep 07	2005 Feb 25	
RX J0438.2+2023	69.55433	20.37975	2004 Sep 07	2005 Feb 25	IRAC C2 with RX J0437.4+1851a
RX J0438.6+1546	69.66279	15.77047	2004 Sep 07	2005 Mar 03	
RX J0439.4+3332a	69.85604	33.54572	2004 Sep 07	2005 Feb 26	
RX J0452.5+1730	73.12812	17.50714	2004 Sep 07	2005 Feb 26	
RX J0452.8+1621	73.20896	16.36922	2004 Sep 07	2005 Feb 26	IRAC C2, MIPS C2 with RX J0452.5+1730
RX J0457.2+1524	74.32358	15.41928	2004 Sep 07	2004 Oct 13	
RX J0457.5+2014	74.37775	20.24158	2004 Sep 07	2004 Oct 13	
RX J0458.7+2046	74.66558	20.77892	2004 Sep 07	2004 Oct 13	IRAC C2 with RX J0457.5+2014
RX J0459.7+1430	74.94237	14.51539	2004 Sep 07	2004 Oct 13	IRAC C2 with RX J0457.2+1524
V836 Tau	75.77746	25.38881	2004 Sep 07	2004 Sep 25	
RX J0902.9−7759	135.71379	−77.99297	2004 Jul 04	2005 Mar 06	
RX J0935.0−7804	143.73350	−78.07203	2004 Jun 10	2004 Jul 09	
RX J0942.7−7726	145.70675	−77.44464	2004 Jun 10	2004 Jul 09	IRAC C2 with RX J0935.0−7804
RX J1001.1−7913	150.28637	−79.21872	2004 May 01	2004 Jul 09	
RX J1150.4−7704	177.61787	−77.07722	2004 May 26	2005 Feb 27	
RX J1216.8−7753	184.19137	−77.89258	2004 May 26	2005 Mar 06	IRAC C3 with RX J1150.4−7704, MIPS C2 with RX J1204.6−7731
RX J1219.7−7403	184.93204	−74.06589	2004 Jul 21	2005 Mar 06	
RX J1220.4−7407	185.09071	−74.12758	2004 Jul 21	2005 Mar 06	IRAC C2 with RX J1219.7−7403
RX J1239.4−7502	189.83850	−75.04419	2004 Jul 21	2005 Mar 06	IRAC C3 with RX J1219.7−7403, MIPS C2 with RX J1220.4−7407
RX J1507.6−4603	226.90725	−46.05433	2004 Jul 20	2005 Mar 09	
RX J1508.6−4423	227.15721	−44.38806	2004 Jul 23	2005 Mar 09	MIPS C2 with RX J1507.6−4603
RX J1511.6−3550	227.90400	−35.84492	2004 Aug 13	2005 Mar 05	
RX J1515.8−3331	228.93904	−33.53325	2004 Jul 20	2005 Mar 05	
RX J1515.9−4418	228.96975	−44.30481	2004 Jul 23	2005 Mar 09	IRAC C2 with RX J1508.6−4423
RX J1516.6−4406	229.15263	−44.12233	2004 Jul 23	2005 Mar 09	IRAC C3 with RX J1508.6−4423
RX J1518.9−4050	229.72008	−40.84800	2004 Jul 24	2005 Mar 06	
RX J1519.3−4056	229.81667	−40.93542	2004 Jul 24	2005 Mar 06	IRAC C2, MIPS C2 with RX J1518.9−4050
RX J1522.2−3959	230.54842	−39.99747	2004 Jul 24	2005 Mar 06	IRAC C3, MIPS C3 with RX J1518.9−4050
RX J1523.4−4055	230.85654	−40.92964	2004 Jul 24	2005 Mar 06	IRAC C4, MIPS C4 with RX J1518.9−4050
RX J1523.5−3821	230.87667	−38.35797	2004 Jul 23	2005 Feb 27	
RX J1524.0−3209	231.01271	−32.16411	2004 Jul 23	2004 Aug 06	
RX J1524.5−3652	231.13483	−36.86742	2004 Jul 24	2005 Mar 05	
RX J1525.5−3613	231.38817	−36.22964	2004 Jul 24	2005 Mar 05	IRAC C2, MIPS C2 with RX J1524.5−3652
RX J1526.0−4501	231.49850	−45.02103	2004 Jul 24	2005 Mar 09	
RX J1538.0−3807	234.51100	−38.12306	2004 Aug 15	2005 Mar 09	
RX J1538.6−3916	234.65946	−39.28203	2004 Aug 15	2005 Feb 27	IRAC C2 with RX J1538.0−3807
RX J1538.7−4411	234.67942	−44.19650	2004 Jul 28	2005 Mar 09	
RX J1540.7−3756	235.17150	−37.93847	2004 Aug 15	2005 Mar 09	
RX J1543.1−3920	235.77600	−39.33872	2004 Aug 15	2005 Mar 09	IRAC C4, MIPS C2 with RX J1538.0−3807
RX J1546.7−3618	236.67171	−36.31311	2004 Aug 12	2005 Mar 05	
RX J1547.7−4018	236.92400	−40.30742	2004 Aug 18	2005 Mar 09	
Sz 76	237.37808	−35.83094	2004 Aug 12	2005 Mar 05	IRAC C2 with RX J1546.7−3618
RX J1550.0−3629	237.49667	−36.49928	2004 Aug 12	2005 Mar 05	IRAC C3 with RX J1546.7−3618
Sz 77	237.94563	−35.94556	2004 Aug 12	2005 Mar 05	IRAC C4 with RX J1546.7−3618, MIPS C2 with RX J1550.0−3629
RX J1552.3−3819	238.08133	−38.32536	2004 Aug 12	2005 Mar 06	IRAC C2 with Sz 82
RX J1554.9−3827	238.72025	−38.46572	2004 Aug 12	2005 Mar 06	IRAC C3 with Sz 82, MIPS C2 with RX J1552.3−3819
RX J1555.4−3338	238.85921	−33.63978	2004 Aug 12	2005 Mar 05	
RX J1555.6−3709	238.89075	−37.16142	2004 Aug 12	2005 Mar 07	IRAC C4 with Sz 82
Sz 81	238.95958	−38.02581	2004 Aug 12	2005 Mar 09	IRAC C5 with Sz 82
RX J1556.1−3655	239.00875	−36.92450	2004 Aug 12	2005 Mar 05	IRAC C6 with Sz 82

TABLE 1—*Continued*

ID	R.A. (deg)	Decl. (deg)	IRAC Observation Date	MIPS Observation Date	Notes[a]
Sz 82	239.03838	−37.93492	2004 Aug 12	2004 Aug 02	
Sz 84	239.51050	−37.60072	2004 Aug 12	2005 Mar 07	IRAC C7 with Sz 82
RX J1559.0−3646	239.74917	−36.77239	2004 Aug 12	2005 Mar 09	
Sz 129	239.81862	−41.95283	2004 Sep 03	2005 Mar 09	
RX J1601.2−3320	240.28733	−33.33725	2004 Aug 13	2005 Mar 07	
RX J1602.0−3613	240.49658	−36.21542	2004 Aug 12	2005 Mar 07	IRAC C3 with RX J1559.0−3646
RX J1603.2−3239	240.79921	−32.65561	2004 Aug 13	2005 Mar 07	
RX J1603.8−3938	240.96875	−39.65036	2004 Sep 03	2005 Mar 09	
RX J1604.5−3207	241.12733	−32.12464	2004 Aug 13	2005 Mar 07	IRAC C2 with RX J1603.2−3239
RX J1605.6−3837	241.38871	−38.62919	2004 Aug 12	2005 Mar 09	
RX J1607.2−3839	241.80708	−38.65661	2004 Aug 12	2005 Mar 09	IRAC C2 with RX J1605.6−3837
RX J1610.1−4016	242.51992	−40.27006	2004 Aug 12	2005 Mar 09	
PZ99 J154920−260005	237.33750	−26.00172	2004 Aug 13	2005 Mar 05	
PZ99 J155506.2	238.77600	−25.35283	2004 Aug 13	2005 Mar 05	
PZ99 J155702−195	239.25975	−19.84497	2004 Aug 12	2004 Aug 04	
PZ99 J160151−244	240.46454	−24.75692	2004 Aug 12	2005 Mar 05	
PZ99 J160158.2	240.49258	−20.13669	2004 Aug 12	2004 Aug 04	
PZ99 J160253.9−2	240.72483	−20.38000	2004 Aug 12	2004 Aug 04	
PZ99 J160550−253	241.46104	−25.55378	2004 Aug 12	2005 Mar 05	
PZ99 J160843−260	242.18083	−26.03800	2004 Aug 12	2005 Mar 05	
PZ99 J161019.1	242.57992	−25.04169	2004 Aug 12	2005 Mar 05	
Wa Oph 1	242.78708	−19.07967	2004 Aug 12	2005 Mar 05	
Wa Oph 2	242.99696	−19.11478	2004 Aug 12	2005 Mar 05	IRAC C2 with Wa Oph 1
RX J1612.0−1906a	242.99696	−19.11478	2004 Aug 12	2005 Mar 05	In FOV of Wa Oph 2
RX J1612.1−1915	243.02217	−19.25550	2004 Aug 12	2005 Mar 05	IRAC C3 with Wa Oph 1
RX J1613.0−4004	243.33112	−40.08633	2004 Aug 12	2005 Mar 09	
RX J1615.3−3255	243.83429	−32.91808	2004 Aug 13	2005 Mar 07	
NTTS 162649−2145	247.45288	−21.86994	2004 Aug 13	2005 Mar 10	
Wa Oph 6	252.19008	−14.27664	2004 Aug 16	2005 Mar 10	

[a] The nomenclature "C*N*" refers to a *Spitzer* cluster target in which one observing template is applied to *N* adjacent sources.

the higher rotational velocities found as young stars contract down toward the main sequence. Follow-up observations on the *ROSAT* samples in these clouds (Taurus, Wichmann et al. 2000; Chamaeleon, Covino et al. 1997; Lupus, Wichmann et al. 1999; Ophiuchus, Martín et al. 1998) verified the presence of strong Li I λ6707 absorption in the *ROSAT* samples. The *Spitzer* WTTS targets were selected from these studies, requiring that the object show Li absorption stronger than that seen in 10^8 Myr Pleiades stars and have spectral types G5 or later where the Li-age relationship is best understood. Brighter objects were favored, as more of them could be observed at the program design sensitivity (see below). WTTSs discovered by earlier surveys in Hα emission, Ca II emission (Herbig & Bell 1988), and by the *Einstein* satellite (e.g., Walter 1986) were also included in the sample. Hα EWs for the WTTS sample range from 9 (in emission) to $\sim$2 Å in absorption. Only about 5% of the sample has Hα in absorption. In addition, seven stars with CTTS Hα characteristics and confused *IRAS*-based SEDs were also included. These are treated separately in our statistics, forming a useful sample of stars with spectroscopic disk indicators for comparison with our WTTSs. A total of 188 objects, spanning spectral types G5–M5, were selected. Results for the first 90 stars of this sample are reported here; the remainder will be discussed in Papers II and III.

2.2. *Spitzer Photometry*

The c2d WTTS observations were carried out with both IRAC (Fazio et al. 2004) and MIPS (Rieke et al. 2004). Target sensitivities for the observations were defined relative to photospheric flux densities; these were estimated by extrapolating optical and NIR photometric measurements into the MIR using a blackbody appropriate to each star's spectral type. The IRAC observations consisted of two 12 s exposures with an offset dither, plus two short 0.6 s exposures ("HDR mode"), taken in both camera fields of view. These achieved sensitivities sufficient to detect the photospheres of all of the targets at S/N $\geq$ 50 in IRAC's broad bands centered at 3.6, 4.5, 5.8, and 8.0 μm. The MIPS 24 μm photometry observations were designed to detect each star's photosphere at S/N = 20. Total exposure times ranging from 42 to 420 s were used, depending on the brightness of each individual target. At 70 μm, the typical stellar flux density of 6 mJy is too faint to readily detect. Most targets were therefore observed at a fixed total exposure time of 360 s. This was sufficient to detect a disk like that of β Pictoris ($L_d/L_* = 10^{-3}$; excess 10 times the photosphere) in the brighter half of the sample and disks 3–10 times more luminous than this in the other half. Thus, only half of our sample has observations with enough 70 μm sensitivity to detect a cold β Pic–like disk.

A list of the targets and observation dates is given in Table 1. Some observations were made in a "cluster" mode combining the data sets from objects located within 1° of each other on the sky. In such cases, the data in the *Spitzer* Science Center Archive can be found by referencing the name of the first target in the cluster. The c2d WTTS data are indexed under *Spitzer* observing program 173, moniker "COREPLANETS_STARS." Enhanced versions of the data products provided by the c2d team can be found online.[9]

Following the observations, the data were processed through the SSC data reduction pipeline version S11.0. The c2d team

[9] See http://data.spitzer.caltech.edu/popular/c2d.

TABLE 2

2MASS AND *Spitzer* PHOTOMETRY

ID	V (mag)	R (mag)	I (mag)	J (mag)	H (mag)	K_s (mag)	$F_{3.6}$ (mJy)	$F_{4.5}$ (mJy)	$F_{5.8}$ (mJy)	$F_{8.0}$ (mJy)	F_{24} (mJy)	F_{70} (mJy)
NTTS 032641+2420	12.20	11.64	11.13	10.32	9.86	9.70	37	25	15	9	0.9	...
RX J0405.3+2009	10.67	9.96	9.41	8.69	8.19	8.09	150	100	67	38	4.3	...
NTTS 040234+2143	14.77	13.72	12.31	10.95	10.29	10.06	31	20	14	9	0.8	...
RX J0409.2+1716	13.44	12.11	11.15	9.96	9.25	9.05	69	48	32	17	1.4	...
RX J0409.8+2446	13.51	12.55	11.35	10.10	9.45	9.25	55	40	26	15	1.9	...
RX J0412.8+1937	12.47	11.68	10.85	9.99	9.43	9.24	52	34	22	12	1.3	...
NTTS 041559+1716	12.23	11.56	10.88	10.03	9.42	9.27	57	37	24	14	1.2	...
RX J0420.3+3123	12.60	11.96	11.30	10.45	9.88	9.73	39	24	15	9	0.9	...
RX J0424.8+2643a	11.35	10.56	9.73	8.61	7.99	7.78	191	152	96	54	5.3	...
RX J0432.8+1735	13.66	12.60	11.32	10.00	9.23	9.02	84	47	37	20	14.3	...
RX J0437.4+1851a	00.00	00.00	00.00	9.42	8.56	8.67	101	61	44	24	2.8	...
RX J0438.2+2023	12.18	11.52	10.90	10.07	9.53	9.36	54	35	21	13	1.1	...
RX J0438.6+1546	10.89	10.31	9.73	8.90	8.36	8.24	134	82	58	34	4.0	...
RX J0439.4+3332a	11.54	10.79	10.13	9.18	8.57	8.42	124	81	51	29	2.9	...
RX J0452.5+1730	11.97	11.08	10.58	9.97	9.41	9.25	56	34	23	14	1.3	...
RX J0452.8+1621	11.74	10.81	10.05	9.10	8.48	8.28	130	97	61	36	3.7	...
RX J0457.2+1524	10.21	9.67	9.13	8.38	7.91	7.75	250	135	95	54	6.5	...
RX J0457.5+2014	11.34	10.73	10.15	9.28	8.82	8.69	93	63	41	23	2.1	...
RX J0458.7+2046	11.95	11.05	10.43	9.59	8.96	8.80	81	53	34	20	2.5	...
RX J0459.7+1430	11.71	11.10	10.53	9.66	9.09	8.95	74	47	31	18	1.5	...
V836 Tau	13.99	12.93	11.74	9.91	9.08	8.60	120	127	107	116	163	120
RX J0902.9−7759	14.01	12.90	11.51	10.10	9.45	9.22	65	42	30	16	2.2	...
RX J0935.0−7804	13.79	12.66	11.21	9.79	9.13	8.89	93	63	40	22	2.3	...
RX J0942.7−7726	13.59	12.64	11.58	10.37	9.68	9.46	47	33	21	12	1.3	...
RX J1001.1−7913	13.23	12.28	11.22	10.07	9.38	9.22	60	41	28	15	1.6	...
RX J1150.4−7704	11.88	11.20	10.62	9.71	9.13	8.97	82	50	32	18	1.9	...
RX J1216.8−7753	14.03	12.94	11.61	10.09	9.46	9.24	59	41	27	15	1.8	...
RX J1219.7−7403	12.93	11.96	11.09	9.75	9.05	8.86	87	58	41	22	2.4	...
RX J1220.4−7407	12.47	11.53	10.64	9.26	8.61	8.37	140	94	62	35	4.1	...
RX J1239.4−7502	10.32	9.75	9.22	8.43	7.95	7.78	194	134	88	51	5.3	...
RX J1507.6−4603	11.69	11.11	10.55	9.82	9.21	9.10	68	46	30	16	1.6	...
RX J1508.6−4423	10.33	9.92	9.65	9.36	8.93	8.81	88	54	36	20	2.0	...
RX J1511.6−3550	12.42	11.74	11.08	10.10	9.52	9.33	55	37	25	13	1.3	...
RX J1515.8−3331	00.00	00.00	00.00	8.98	8.46	8.38	118	80	52	28	3.3	...
RX J1515.9−4418	12.47	11.81	11.17	10.18	9.57	9.45	47	29	20	12	1.1	...
RX J1516.6−4406	11.99	11.35	10.77	9.90	9.32	9.19	53	37	25	14	1.4	...
RX J1518.9−4050	10.90	10.39	9.88	9.14	8.66	8.55	112	68	47	27	2.6	...
RX J1522.2−3959	12.08	11.42	10.77	9.91	9.30	9.10	64	44	28	17	1.6	...
RX J1523.4−4055	11.95	11.34	10.76	9.96	9.39	9.26	57	37	25	14	1.2	...
RX J1523.5−3821	14.24	13.18	11.83	10.40	9.70	9.50	48	33	23	13	1.5	...
RX J1524.0−3209	12.36	11.52	10.60	9.50	8.82	8.64	106	70	47	24	2.7	...
RX J1524.5−3652	10.84	10.35	10.03	9.55	9.05	8.93	81	48	32	18	1.8	...
RX J1526.0−4501	10.95	10.48	10.05	9.44	8.98	8.90	75	48	32	18	1.6	...
RX J1538.0−3807	12.32	11.62	10.95	10.11	9.57	9.38	52	35	23	13	1.3	...
RX J1538.6−3916	11.60	11.00	10.41	9.59	9.01	8.85	80	50	32	18	1.8	...
RX J1538.7−4411	10.47	9.99	9.51	8.80	8.34	8.21	134	88	59	33	4.7	...
RX J1540.7−3756	12.19	11.45	10.94	9.93	9.32	9.19	61	37	24	15	1.3	...
RX J1546.7−3618	11.39	10.85	10.28	9.49	8.95	8.78	97	56	40	23	2.0	...
RX J1547.7−4018	11.06	10.51	10.00	9.29	8.81	8.66	87	60	42	22	1.9	...
Sz 76	15.15	13.98	12.45	10.96	10.28	10.02	34	26	22	28	64	120
RX J1550.0−3629	00.00	00.00	00.00	9.56	9.02	8.88	76	52	36	20	1.9	...
Sz 77	12.11	11.29	10.50	9.44	8.59	8.27	223	181	160	189	343	110
RX J1552.3−3819	13.08	12.23	11.41	10.36	9.68	9.53	45	30	19	11	1.1	...
RX J1554.9−3827	13.43	12.53	11.57	10.41	9.74	9.57	47	31	21	12	1.2	...
RX J1555.6−3709	12.39	11.65	10.94	9.96	9.33	9.16	64	40	27	15	1.2	...
Sz 81	14.87	13.53	11.78	10.18	9.53	9.17	89	67	72	71	79.4	110
RX J1556.1−3655	13.37	12.57	11.65	10.40	9.60	9.30	82	72	55	62	171	154
Sz 82	11.85	11.01	10.13	8.78	8.09	7.74	315	284	277	380	648	987
Sz 84	16.13	14.70	12.88	10.93	10.20	9.85	42	29	20	12	20.9	244
RX J1559.0−3646	13.50	12.51	11.31	10.14	9.46	9.28	67	43	30	17	1.5	...
Sz 129	12.93	12.07	11.13	9.93	9.08	8.61	170	159	130	165	274	254
RX J1601.2−3320	11.06	10.50	9.91	9.03	8.55	8.53	108	68	46	30	3.2	...
RX J1602.0−3613	11.87	11.22	10.53	9.60	8.97	8.85	85	61	38	22	2.1	...
RX J1603.2−3239	12.71	11.90	11.05	9.98	9.29	9.12	67	46	32	18	8.3	...
RX J1607.2−3839	12.72	11.85	10.93	9.69	8.96	8.88	88	55	39	23	2.4	...

TABLE 2—*Continued*

ID	V (mag)	R (mag)	I (mag)	J (mag)	H (mag)	K_s (mag)	$F_{3.6}$ (mJy)	$F_{4.5}$ (mJy)	$F_{5.8}$ (mJy)	$F_{8.0}$ (mJy)	F_{24} (mJy)	F_{70} (mJy)
RX J1610.1−4016	11.18	10.61	10.06	9.34	8.80	8.62	98	69	46	26	2.8	...
PZ99 J154920−260	00.00	10.35	9.71	8.64	8.13	7.91	184	117	80	47	4.4	...
PZ99 J155506.2	12.30	11.42	10.52	9.41	8.62	8.51	123	80	52	29	2.9	...
PZ99 J155702−195	00.00	11.01	10.24	9.18	8.49	8.37	141	91	61	34	3.2	...
PZ99 J160151−244	00.00	11.38	10.54	9.41	8.66	8.48	122	74	52	29	3.0	...
PZ99 J160158.2	10.45	9.87	9.27	8.35	7.81	7.67	199	147	106	60	6.2	...
PZ99 J160253.9−2	00.00	11.54	10.58	9.16	8.46	8.19	158	115	85	44	4.8	...
PZ99 J160550−253	00.00	10.46	9.99	9.11	8.59	8.46	105	76	49	28	3.1	...
PZ99 J160843−260	00.00	10.01	9.30	8.55	8.05	7.91	197	125	86	47	4.9	...
PZ99 J161019.1	11.89	11.06	10.27	9.25	8.54	8.36	121	83	57	32	3.9	...
Wa Oph 1	11.98	11.11	10.17	8.76	7.98	7.69	282	174	117	66	7.1	...
Wa Oph 2	11.69	10.96	10.35	8.98	8.32	8.09	127	102	69	38	5.0	...
RX J1612.1−1915	13.57	12.55	11.47	10.05	9.08	8.86	90	52	39	21	1.8	...
RX J1613.0−4004	00.00	00.00	00.00	10.47	9.44	9.11	72	43	31	18	1.9	...
RX J1615.3−3255	12.04	11.28	10.54	9.44	8.78	8.56	114	85	61	66	271	727
Wa Oph 6	13.22	12.02	10.79	8.72	7.57	6.86	1018	924	871	814	1054	989
RX J1519.3−4056	11.44	10.84	10.27	9.55	9.02	8.83	90	58	37	21	2.1	...
RX J1525.5−3613	11.64	11.04	10.44	9.56	9.00	8.84	74	58	38	22	2.1	...
RX J1543.1−3920	12.20	11.48	10.79	9.85	9.21	9.10	62	43	29	16	1.3	...
RX J1555.4−3338	12.48	11.77	11.06	10.16	9.54	9.35	49	34	23	13	1.6	...
RX J1603.8−3938	11.23	10.58	9.90	8.94	8.36	8.22	149	93	63	35	3.5	...
RX J1604.5−3207	10.81	10.29	9.79	9.17	8.69	8.56	119	73	49	28	2.7	...
RX J1605.6−3837	14.24	13.22	12.05	10.79	10.10	9.90	37	23	16	9	1.0	...
RX J1612.0−1906a	11.60	10.87	10.10	8.98	8.32	8.09	127	102	69	38	5.0	...
NTTS 162649−2145	11.06	10.32	9.81	8.68	8.00	7.76	248	153	104	57	6.2	...

NOTES.— Photometric measurement uncertainties are estimated at 1% for 2MASS, 15% for IRAC and MIPS-24, and 20% for MIPS-70. Absolute calibration uncertainties are discussed in the text.

then applied a number of algorithms designed to mitigate remaining instrumental signatures (Young et al. 2005). The WTTSs were located on the images using Two Micron All Sky Survey (2MASS) positions, which in some cases are offset by 20″–40″ from the *ROSAT* positions reported in the literature. Pointing for IRAC is offset from 2MASS by a fraction of an arcsecond, while MIPS 24 μm pointing is reliable to within 2″ (Fazio et al. 2004; Rieke et al. 2004). Point-spread function (PSF) fitting photometry was performed on the mosaicked images using the "cd2phot" code adapted by the c2d team (Young et al. 2005; Harvey et al. 2006). Photometric measurement uncertainties of about 2% are typical for moderately bright IRAC and MIPS-24 sources. The absolute calibration errors are estimated at approximately 5% for IRAC and 7% for MIPS-24 (SSC Data Handbook). Unlike the other bands, photometry for MIPS-70 detections has been measured using aperture photometry on the filtered SSC post-BCD mosaics. For these preliminary photometric measurements, uncertainties are estimated at 30%. A forthcoming paper will contain improved 70 μm photometry and rigorous upper limit estimates for the 70 μm fluxes of these sources. Bright sources in any of the bands may have a higher uncertainty due to PSF fitting problems and latent image effects. Table 2 presents the optical through 70 μm photometry for our sources.

2.3. *Optical Photometry*

In order to construct SEDs using contemporaneous optical, NIR, and MIR data, *VRI* optical observations of the Taurus objects were made with the 0.8 m telescope at McDonald Observatory on five different photometric nights during two observing runs in 2003 December and 2004 January. The southern targets were observed with the 0.9 m telescope at Cerro Tololo Inter-American Observatory during four photometric nights in 2004 May. In addition to the program stars, on each night, three fields of Landolt standards (approximately five standards per field) were observed at different air masses. We tailored our exposure times to obtain excellent S/N in every observation. The standard IRAF packages CCDRED and DAOPHOT were used to reduce the data and perform aperture photometry. The rms scatter of the photometric solutions applied to the programs stars was 0.01–0.02 mag in all three filters. We adopt a conservative photometric error of 0.02–0.03 mag.

3. RESULTS

3.1. *Frequency of Excess Emission*

Due to uncertainties in extinction, spectral types, and absolute photometry, relative photometric colors are used for detecting excess emission. This technique has been widely utilized by *Spitzer* researchers to reveal IR excesses in young stars (Gorlova et al. 2004; Rieke et al. 2005; Beichman et al. 2005). We have chosen to identify excesses at 8 and 24 μm using the $K_s - [24]$ and $K_s - [8]$ color. These colors are approximately zero for Rayleigh-Jeans photospheres in spectral types earlier than late M (Gorlova et al. 2004). Figure 1 shows a plot of 2MASS K_s magnitude versus $K_s - [24]$ color for our 90 star sample. The sample is dominated by the locus of points with $K_s - [24]$ approximately zero. This group of sources spans brightnesses from $K_s = 8$ to 11, covering our range of spectral types in nearby clouds. The width of this distribution is $\approx$0.2, indicating the minimal photometric errors in our data set. Substantial K-band extinction might also tend to produce red $K_s - [24]$ colors. However, published A_v for these stars indicate very low NIR extinctions for most of the sources. In addition, Figure 2 plots $H - K_s$ versus $K_s - [24]$, and the reddening vector for $A_v = 5$ demonstrates that even high extinction cannot produce excess sources on our color-magnitude diagram

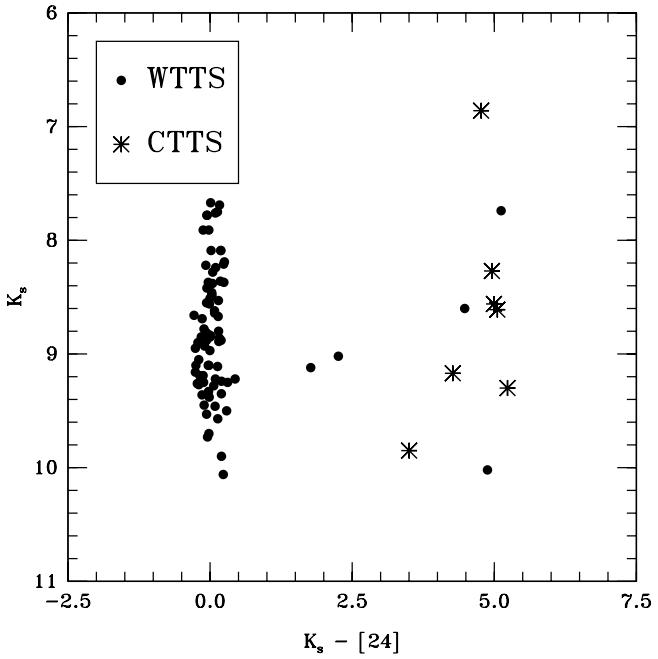

FIG. 1.—K_s vs. $K_s - [24]$ for 90 young stars with low and moderate Hα emission.

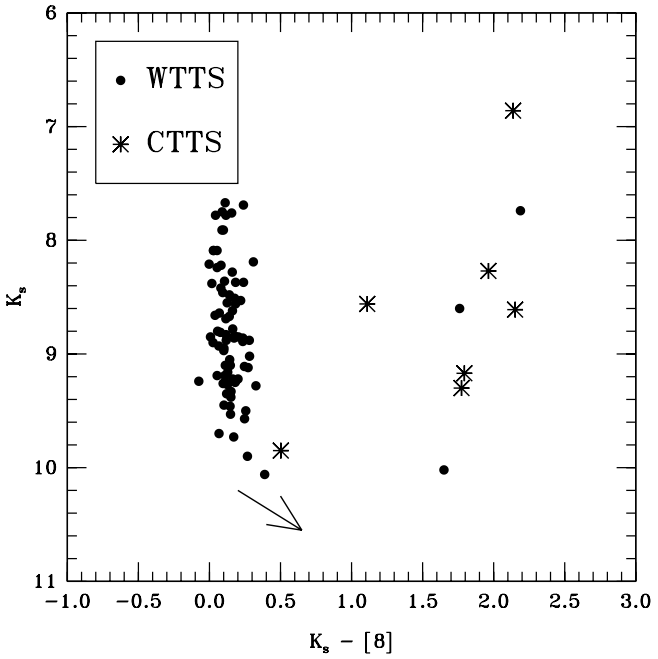

FIG. 3.—K_s vs. $K_s - [8]$ for 90 young stars with low and moderate Hα emission. The reddening vector is for $A_v = 5$.

since the principal displacement is perpendicular to the $K_s - [24]$ axis. Twelve sources are located 1–3 mag redward of the photospheric locus. These are the stars for which we detect excess emission at 24 μm. Seven of these stars are CTTSs; only five are WTTSs. Interestingly, the only sources obviously detected at 70 μm are the ones with 24 μm excesses. Thus, unlike surveys of older stars in the solar neighborhood for which 70 μm excesses are fairly common (Bryden et al. 2006), we have thus far found no young stars with obvious excess only at $\lambda \geq 70$ μm. However, we emphasize that unlike our observations, the Bryden et al. (2006) 70 μm sensitivity limit reaches the stellar photosphere for all their targets. Figure 3 presents a similar plot for $K_s - [8.0]$. Out of 90 stars, nine stars (3/83 WTTSs; 6/7 CTTSs) show excess at 8 μm. Three stars with 24 μm excess lack 8 μm excess. Of these, two are WTTSs. The third is the low-luminosity CTTS Sz 84. Our minimal group of seven CTTSs has a 100% excess detection rate at 24 and 70 μm. On the other hand, only 5 out of 83 (=6%) of the stars with Hα EW $\leq$ 10 Å in emission have a detectable excess at 24 or 70 μm. SEDs for WTTSs with excess emission are presented in Figure 4. SEDs for CTTSs may be found in Figure 5. These SEDs are constructed from our optical *VRI* photometry, 2MASS *JHK* photometry, *Spitzer* IRAC (3.6, 4.5, 5.8, and 8.0 μm), and *Spitzer* MIPS (24 and 70 μm). Note that the photospheric models have been normalized to *I* band.

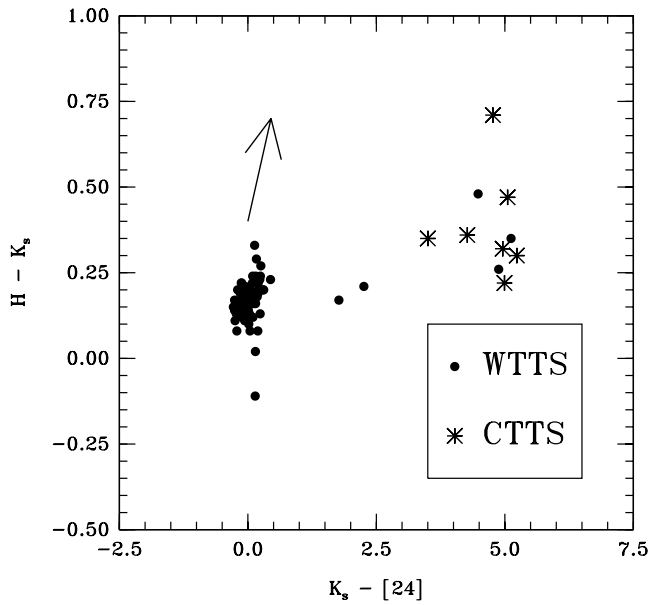

FIG. 2.—$K_s - H$ vs. $K_s - [24]$ for 90 young stars with low and moderate Hα emission. The reddening vector is for $A_v = 5$. This plot shows that high-extinction sources will not be confused with 24 μm excess sources.

3.2. *Fractional Disk Luminosities*

Table 3 contains fractional disk luminosities L_d/L_* for the excess sources. Within our sample of excess objects, L_d/L_* ranges from 0.19 to 0.008. Our CTTS disk values range from 0.19 to 0.05. On the other hand, the famous debris disk β Pic has a fractional luminosity of only 0.002 (Backman & Paresce 1993). One unusual CTTS (Sz 84) has an exceptionally small $L_d/L_* < 0.001$. It is discussed in § 3.3.6. Three of the WTTSs with disks have luminosities consistent with the lowest part of the CTTS range. The remaining two WTTS disks are almost an order of magnitude less luminous than the other sources. Their L_d/L_* falls squarely between the Class II and debris disk range, filling an important gap in our knowledge of disk evolution.

3.3. *Objects with Excess Emission*

3.3.1. *RX J0432.8+1735*

RX J0432.8+1735 is a *ROSAT*-detected star near the Taurus star formation region at a distance of 140 pc. This object was first reported by Carkner et al. (1996) as a strong X-ray source in an 8 ks pointed *ROSAT* observation that was subsequently identified as an M-type weak Hα emission star in the L1551

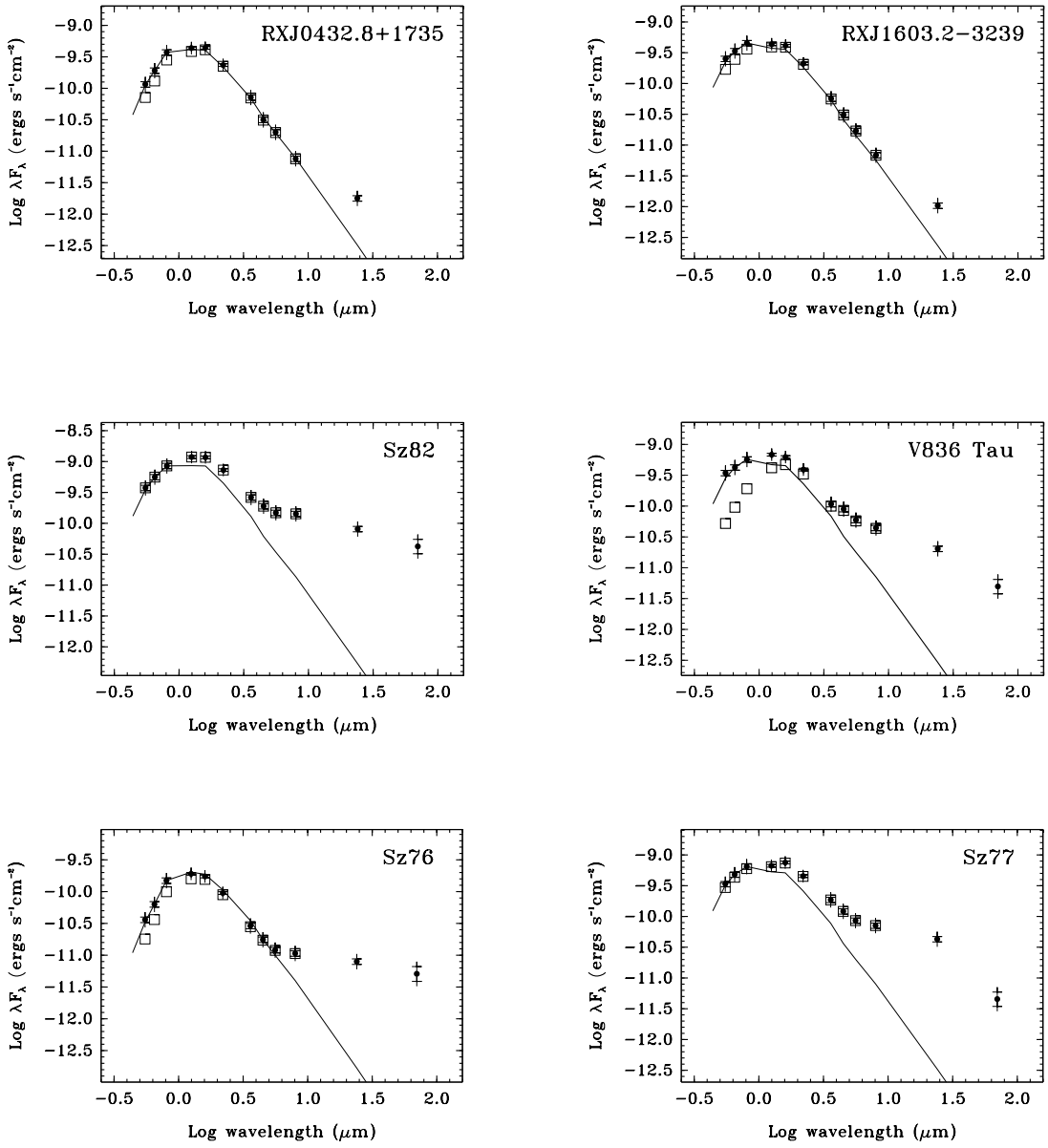

FIG. 4.—SEDs and model photospheres for WTTSs with excess. Points are plotted for optical photometry, 2MASS, IRAC, and MIPS. Dereddened fluxes are indicated by squares. Model photospheres based on the published spectral types for each star are shown for comparison.

cloud. Wichmann et al. (1996) reported a spectral type of M2 and an Hα EW of 1.7 Å in emission. Undetected to a limit of 0.19 mJy at 8.4 GHz in a radio survey by Carkner et al. (1997), RX J0432.8+1735 was also observed using speckle interferometry by Kohler & Leinert (1998), who found no companions down to $\Delta K \approx 3$ at 0.″13. Martín & Maguzzù (1999) obtained high-resolution spectroscopy, confirming this star's spectral type and low Hα EW, as well as showing that its lithium EW places it squarely in the WTTS regime. Hanson et al. (2004) determined proper motions of $\alpha = 11.3$ mas yr^{-1}, $\delta = -19$ mas yr^{-1}; a similar value was found by Ducourant et al. (2005), consistent with the CTTS GG Tau, which is only 7′ away. The proximity of RX J0432.8+1735 to this 1.5 Myr circumbinary disk source also provides evidence of its young age (White et al. 1999). The PMS tracks of D'Antona & Mazzatelli (1997, hereafter DM97) yield an age of 1 ± 0.5 Myr. The SED is presented in Figure 4. All of the *Spitzer* photometry points fall very close to the photosphere with the exception of MIPS 24 μm. The 24 μm flux is a factor of 3 above the expected photospheric value and is detected at a high S/N level. There was no detection of MIPS 70 μm for this source.

3.3.2. *RX J1603.2−3239*

RX J1603.2−3239 is a young star in the Lupus star-forming region at a distance of ∼150 pc (Sartori et al. 2003). This object was first reported as a K7 X-ray–bright star with Hα EW = 1.13 Å in emission (Krautter et al. 1997). The star has a photometrically determined rotation period of 2.77 days with an amplitude of 0.11 mag in V (Wichmann et al. 1998). Shortly thereafter, Wichmann et al. (1999) performed high-resolution spectroscopy on this star, confirming its lithium EW in excess of Pleiades values for its spectral class and showing a significant central absorption in its Hα emission, which indicates a nonchromospheric origin for this line. Sartori et al. (2003) report $A_v = 0.49$ and derive $\log L_* = -0.40$ based on a distance for nearby *Hipparcos*-detected early-type stars. The DM97 tracks indicate an age of 1.7 ± 0.4 Myr. Our SED (Fig. 4) shows all IRAC photometric points lying near the photosphere. However, the 24 μm flux is a

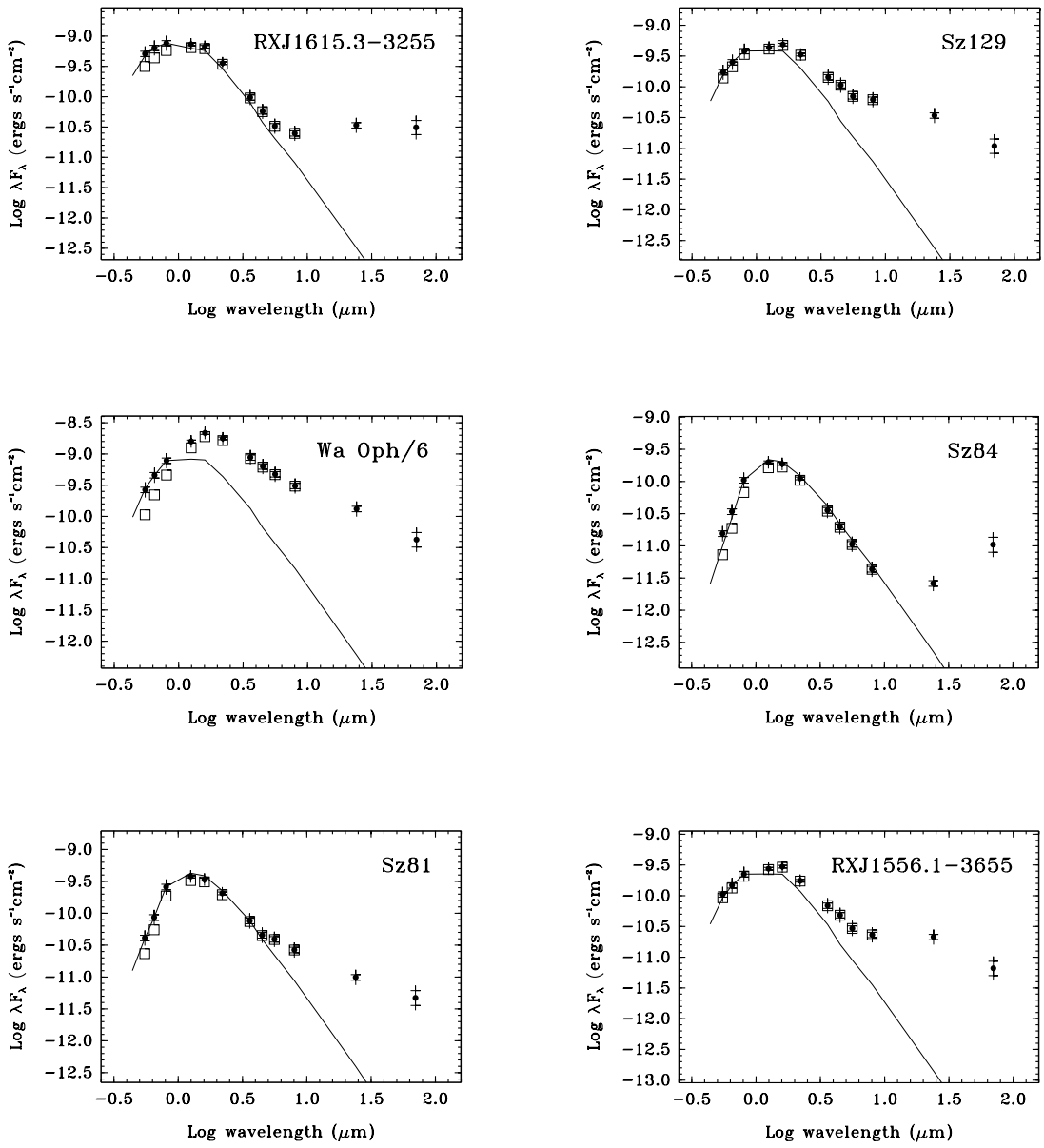

FIG. 5.—SEDs and model photospheres for CTTSs. Points are plotted for optical, 2MASS, IRAC, and MIPS photometry; dereddened fluxes are indicated by squares. Model photospheres based on the published spectral types for each star are shown for comparison.

TABLE 3
FRACTIONAL DISK LUMINOSITIES

Star	L_d/L_*	CTTS / WTTS
Wa Oph 6	0.19	CTTS
RX J1556.1−3655	0.10	CTTS
Sz 81	0.05	CTTS
Sz 129	0.11	CTTS
Sz 84	∼0.0008	CTTS?
RX J1615.3−3255	0.08	CTTS
Sz 77	0.11	CTTS
Sz 76	0.10	WTTS
Sz 82	0.12	WTTS
V836 Tau	0.11	WTTS
RX J0432.8+1735	∼0.01	WTTS
RX J1603.2−3239	∼0.01	WTTS

factor of 3 above the predicted photospheric value. Like RX J0432.8+1735, this source appears to have an SED consistent with a tenuous disk that has a large inner hole.

3.3.3. *V836 Tauri*

V836 Tauri is a K7 star in the western part of the Taurus star-forming region near L1544. A thorough review of its optical photometric and spectroscopic properties is presented in White & Hillenbrand (2004). Its Hα EW in that work is cited as 25 Å although the HBC (Herbig & Bell 1988) gives the emission strength as 9 Å (Mundt et al. 1983). An even lower value of 4.4 Å with an inverse P Cygni profile was reported by Wolk & Walter (1996). These measurements classify V836 Tau as a borderline WTTS/CTTS. V836 Tauri and LkCa 15 were the only WTTSs detected in the millimeter continuum and CO survey of Duvert et al. (2000) and are two of the few WTTSs detected in the millimeter continuum by Osterloh & Beckwith (1995). V836 Tauri is sometimes claimed as an "older" T Tauri star due to derived ages in excess of 7 Myr (Strom et al. 1989); however, Hartmann

(2003) casts some doubt on the accuracy of such model-dependent estimates. V836 Tauri has a faint nearby companion that is likely a background star (Massarotti et al. 2005). Despite the weak Hα emission, *IRAS* strongly detected excess emission from this star at all four bands (Wolk & Walter 1996; Kenyon & Hartmann 1995). Our dereddened SED (Fig. 4) shows a modest amount of excess emission in the NIR, almost none at 3.6 μm, and an increasing amount in the IRAC and MIPS bands. The excess emission in this source has been fitted with an optically thick disk, most recently by Andrews & Williams (2005), who found a disk mass of 0.01 $M_{\odot}$. Thus, although V836 Tau has strongly variable Hα, it has excesses typical for a CTTS, although it shows little excess in the NIR bands.

3.3.4. *Sz 82*

Sz 82, also known as IM Lupi, is an M0 star in the Lupus star-forming region. The Hα emission is known to vary from 7.5 to 21.5 Å, confirming its status as a borderline WTTS/CTTS. Although Sz 82 has not been observed by a millimeter interferometer, it is detected strongly in the 1.3 mm continuum (260 mJy; Nürnberger et al. 1998). The Sz 82 disk has been resolved in scattered light by the *Hubble Space Telescope* (*HST*; Padgett et al. 1999, 2004). Like V836 Tau, this source was detected by *IRAS* (Carballo et al. 1992). Our SED (Fig. 4) shows a modest NIR excess that begins to increase at 5.8 μm and is nearly flat between 8 and 70 μm. A simple disk model for this object's SED is presented in § 4.2.

3.3.5. *Sz 76*

Sz 76, an M1 star in Lupus, is another borderline WTTS/CTTS with an Hα EW = 10.3 Å (Hughes et al. 1994). The source was detected in X-rays during a pointed *ROSAT* observation of Lupus I (Krautter et al. 1997). It was not seen at 1.3 mm down to a detection limit of 45 mJy, which constrains its cold disk mass to $\leq 5 \times 10^{-3}$ $M_{\odot}$ (Nürnberger et al. 1997). Although no *IRAS* detections have been reported for this source due to this mission's limited sensitivity, we find substantial excess emission for this star longward of 4.5 μm (Fig. 4). A preliminary effort to model the possible disk of Sz 76 is reported in § 4.2.

3.3.6. *Classical T Tauri Stars*

Seven CTTSs either without *IRAS* detections or with confused *IRAS* SEDs were included in our sample. These vary in Hα properties from the borderline WTTS/CTTS Sz 77 [EW(Hα) = 12 Å; Hughes et al. 1994] to RX J1556.1−3655 [EW(Hα) = 83 Å; Wichmann et al. 1999]. The SEDs of the CTTSs are presented in Figure 5 with the exception of Sz 77, which is in Figure 4. A wide variety of SED morphologies are displayed by these sources. The most extreme levels of excess emission from 1.2 to 70 μm are shown by Wa Oph 6, a K6 star with EW(Hα) = 35 Å (Walter 1986). On the other hand, Sz 84, an M5.5 star with EW(Hα) = 44 Å, has almost no measurable excess shortward of 24 μm, implying a sizable disk inner hole. The K5 star RX J1615.3−3255 [EW(Hα) = 19 Å] also has very little excess shortward of 8 μm. Thus, within our very limited sample, Hα EWs do not appear to correlate with the presence of infrared excess, although it seems that IR excess is rare among stars with Hα EW $\leq$ 10 Å. This finding appears to extend to somewhat below the WTTS defining level of 10 Å Hα emission since the three borderline WTTSs/CTTSs in our sample show disk emission that is indistinguishable from the CTTSs in our sample.

The purported CTTS Sz 84 merits additional consideration due to its very low fractional disk luminosity of $<$0.001. Because of its relatively high Hα EW, this source was listed as a Lupus T Tauri star in Schwartz (1977). However, it was not included in Herbig & Bell (1988) despite being discovered well in advance of this seminal work. Its long pedigree and faint visual magnitude of 16.2 (Hughes et al. 1994) have apparently caused it to be overlooked entirely in Li I λ6707 EW determinations. Sz 84 also stands out as the star with the lowest $N_{\rm H}$ determined from *ROSAT* observations in Krautter et al. (1997). It has a column density of hydrogen that is considerably lower than the bulk of stars in Lupus ($\log N_{\rm H} \sim 18$ vs. 21). Although its estimated age on the DM97 tracks is 1.0 $\pm$ 0.3 Myr, its age is entirely dependent on placing the object at the distance of the cloud. A young main-sequence star in the foreground would also be consistent with the photometry and low $A_v \approx 0$ (Hughes et al. 1994). Given the tendency of main-sequence late M stars to have strong Hα lines, the low disk luminosity, and the $N_{\rm H}$ value that is suggestive of a foreground object, it is necessary to question the CTTS identity of Sz 84. Observations of the Li I λ6707 line will settle the question of whether this source is a foreground young star with a debris disk such as St 34 in Taurus (Hartmann et al. 2005b).

4. DISCUSSION

4.1. *Disks, Companions, or Extragalactic Confusion?*

Two of the WTTSs in our survey show excesses only at 24 μm. Although we are inclined to attribute this excess to dust emission in a disk due to analogy with CTTSs, it is also conceivable that excesses could be caused by an unresolved nearby source. The MIPS 24 μm PSF has an FWHM of 5.″7, larger than the IRAC PSFs by a factor of 2. Thus, it is possible that a nearby source could be blended into the PSF at the longer wavelength. However, in neither case is there an obvious IRAC source near the position of the 24 μm source. An exact overlap with an extragalactic interloper is also a possibility, although the areal density of these sources is only 300 deg^{-2} for fluxes $\geq$1 mJy (Papovich et al. 2004). Given a random distribution of galaxies, the probability of having one source with a superposition in the 6″ MIPS 24 μm beam is 0.065%. Thus, in our list of 90 stars, there is about a 6% probability of a chance superposition or 0.138% for two superpositions. It is also true that by selecting for X-ray-bright stars, we may also be selecting for X-ray–bright active galactic nuclei that are also bright at 24 μm (Franchesini et al. 2005). Most extragalactic sources have relatively flat spectra between 8 and 24 μm (Rowan-Robinson et al. 2005), and the sensitivity of IRAC is higher than MIPS, so extragalactic interlopers would likely be detected at the IRAC bands as well as 24 μm. Unfortunately, the brightness of the stellar photosphere in the IRAC bands will likely drown out the extragalactic component. It is at 24 μm for stars with photospheric levels of $\approx$1 mJy that this problem is most likely, as in our survey. Unfortunately, very high resolution imaging at high contrast will be required to completely rule out this conundrum for low-luminosity WTTS disks. A final possibility is the presence of a low-mass stellar companion that is unresolved even at optical wavelengths. Due to the shape of the possible companion SED, it is highly unlikely that such a source would be undetected at 8 μm. These purported companions would have to be 3 times as bright as the primary at 24 μm but less than 10% as bright at 8 μm to fulfill the SED requirements. The only plausible stellar companion of this sort would be obscured by an edge-on disk and visible only in scattered light shortward of 10 μm, as in the case of HV Tau C, where an edge-on disk is an optical companion of a WTTS binary (Hartmann et al. 2005a).

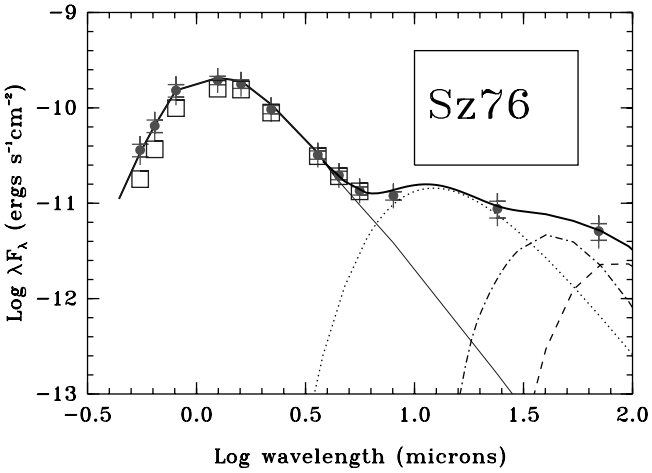

FIG. 6.—Sz 76 SED and disk model. The thick solid line indicates the integrated model flux. The thin solid line shows the stellar photosphere. The dotted line represents the contribution from the disk inner rim, the dot-dashed line represents the disk photosphere, and the dashed line represents the disk interior flux. [*See the electronic edition of the Journal for a color version of this figure*.]

4.2. *Comparison to Disk Models*

In order to investigate the physical parameters of the WTTS disks identified in § 3, we compare their SEDs to disk models. We use the passive disk model presented by Dullemond et al. (2001), which is based on the Chiang & Goldreich (1999) flared disk model but includes an evacuated inner cavity and an inner rim. The specific application of the Dullemond model to T Tauri stars (rather than Herbig Ae/Be stars) has been called into question recently by Vinkovic et al. (2006) and Isella & Natta (2005). However, in the current case, this model is only used to provide preliminary insight into possible disk structures. It is entirely likely that more conventional T Tauri disk models (e.g., D'Alessio et al. 2005) would also fit the data, potentially requiring smaller inner disk holes. In the context of this model, the SED of an object can be constructed from the superposition of the flux contributions of four different components: the stellar photosphere, an inner rim, the disk's surface layer, and the disk's midplane. Figures 6–8 show the SEDs and disk models for the PMS stars Sz 76, Sz 82, and Sz 84. As described in § 3.2, Sz 76 and Sz 82 are two borderline WTTSs/CTTSs, while Sz 84 is a purported CTTS with no measurable excess at IRAC wavelengths (although it shows large 24 and 70 μm excesses). The stellar and disk model parameters are listed in Table 4. The stellar $T_{\rm eff}$ and luminosity were derived as described in § 4.4. The stellar masses come from the evolutionary tracks by Siess et al. (2000, hereafter S00). The free parameters fitted to the disk models are disk mass, inner and outer radii, inclination, and the power index of the surface density of the disk (although the latter two parameters are not well constrained by the data). We find that for these particular models, the excesses at IRAC wavelengths are completely dominated by the blackbody emission from the inner rim. Therefore, the inner radius and the inclination of the disk are relatively well constrained by the relative intensities and magnitude of the IRAC excesses. The total mass of the disk, the outer radius, and the power index are degenerate parameters only partially constrained by the 24 and 70 μm fluxes. These are very preliminary results, but they show that the SEDs of WTTSs can be well reproduced by simple passive flared disk models with large inner holes.

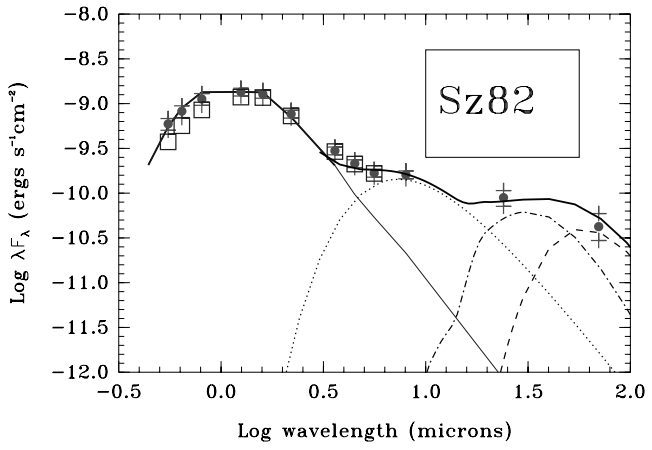

FIG. 7.—Sz 82 SED and model as in Fig. 6. [*See the electronic edition of the Journal for a color version of this figure*.]

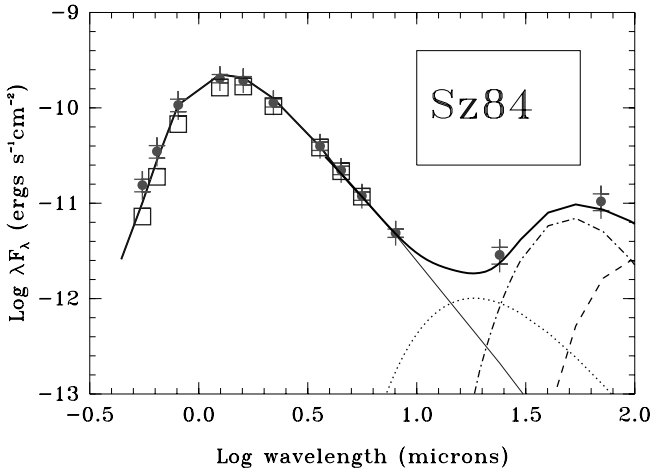

FIG. 8.—Sz 84 SED and model as in Fig. 6. [*See the electronic edition of the Journal for a color version of this figure*.]

4.3. *Disks Are Rare among WTTSs*

If the low frequency of disks among WTTSs is confirmed by the remainder of the c2d WTTS survey, it appears that most weak-line T Tauri stars are indeed "naked" T Tauri stars at circumstellar radii less than those probed by 24 μm emission. A substantial population of stars apparently coeval with the CTTSs have fully disposed of their inner and outer disks within a time frame of a few million years. These results are similar to those found by Hartmann et al. (2005a) for WTTSs in Taurus-Auriga. These authors found that the [3.6]−[4.5] versus [5.8]−[8.0] diagram clearly separates the bulk of CTTSs (IRAC excess sources) from WTTSs (nonexcess sources) with a few ambiguous cases such as CoKu Tau 4, which has excess only beyond 15 μm. However, the present study extends these conclusions beyond 8 μm to include the outer disks probed by 24 and 70 μm. Another IRAC

TABLE 4
MODEL PARAMETERS

Star	L_* ($L_\odot$)	$T_{\rm eff}$ (K)	M_* ($M_\odot$)	$M_{\rm disk}$ ($M_\odot$)	$R_{\rm in}$ (AU)	$R_{\rm out}$ (AU)	Inclination (deg)	psig[a]
Sz 76	0.25	3580	0.35	1.2×10^{-3}	1.0	105	10	−2
Sz 82	1.65	3850	0.60	5.0×10^{-4}	0.5	150	25	−1.5
Sz 84	0.35	3370	0.30	1.5×10^{-4}	3.0	250	0.5	−2

[a] Power index (exponent) of the surface density of the disk.

excess survey among young stars 3–30 Myr in age is reported by the FEPS group (Silverstone et al. 2006). These authors found that 5/74 sources possess infrared excesses and 4 of these have ages estimated in the 3–10 Myr range. Interestingly, three of their five excess stars would be classified as CTTSs based on their Hα EW. A few *Spitzer* excess surveys of slightly older stars have also been published recently. Among the 23 G–M-type members of the TW Hya association with an age of about 10 Myr, the 24 μm excess fraction is about 20% (Low et al. 2005). However, only one of the solar-type excess objects qualifies as a CTTS based on spectroscopic criteria (Webb et al. 1999). An even higher excess fraction (40%) was found in the 8–10 Myr η Cha association, but five out of six excess stars are CTTSs (Megeath et al. 2005). A similar fraction (35%) has been found for the F- and G-type stars in Upper Sco-Cen (Chen et al. 2005). Notably, our excess fraction of 6% is considerably lower than the 20% excess fraction among A stars with ages of 5 Myr or less (Rieke et al. 2005), but these sources are not sorted by emission-line brightness as in our survey. The study of Tr37 by Sicilia-Aguilar et al. (2006) find a 7% excess frequency among their WTTS. However, Lada et al. (2006) find a much higher fraction of disks (34%) among the WTTS in IC 348. Their sample includes many late M stars, unlike the current study, and suggests that main-sequence contamination of the current sample may be an issue. *IRAS* and *ISO* studies of WTTS mid-infrared excess are not sensitive enough to reach the photosphere at 24 μm, so they are unable to identify more than just the optically thick disk population (e.g., Gras-Velázquez & Ray 2005). For a similar reason, it is important to note that some faint WTTSs may have outer disks that remain undetected by *Spitzer* due to the lower than expected sensitivity of the MIPS 70 μm channel and the brightness of background nebulosity at that wavelength. Unfortunately, the time required for *Spitzer* to detect the photosphere of every WTTS at 70 μm would be prohibitive. The old but nearby solar neighborhood population has been surveyed by *Spitzer* at 70 μm to much greater depth than our survey, possibly accounting for its higher detection rate of cold disks (Bryden et al. 2006). Based on the 24 μm and IRAC excess statistics, the frequency of excess among WTTSs is lower than any other group of young sources up to ages of 10 Myr, but it is higher than the approximately 1% 24 μm excess frequency among main-sequence populations (Bryden et al. 2006). We confirm and extend the findings of previous researchers that lack of significant Hα emission among young solar-type stars indicates a lack of disk material even at a very tenuous level for $r < 3$ AU.

4.4. *Optically Thin T Tauri Star Disks?*

Two of the objects in our survey have derived fractional disk luminosities that are among the lowest yet detected by *Spitzer* for very young stars. In order to have a fractional luminosity of 1%, an optically thick disk must be extremely flat and thin to intercept such a small percentage of the stellar luminosity (Chen et al. 2005; Kenyon & Hartmann 1987). On the other hand, these disks could be optically thin, in which case their L_d/L_* of 0.01 would have approximately 10 times the fractional disk luminosity of the β Pic disk. If the excesses of RX J0432.8+1735 and RX J1603.2−3239 are not due to a chance extragalactic superposition, they are possibly the first optically thin disks discovered around very young T Tauri stars. At a brightness 10 times that of β Pic, such disks should be easily visible with high-contrast observations using *HST*.

4.5. *Foreground Contamination by Young Main-Sequence Stars*

One caveat to the above conclusion is continuing uncertainty as to the contamination of the WTTS sample by ~100 Myr old field stars (Covino et al. 1997). A recent astrometric evaluation of *ROSAT*-selected young stars around Tau-Aur concludes that the sample is heterogeneous, consisting of a few actual Tau-Aur association members mixed with Pleiades supercluster stars, Hyades cluster members, and other foreground young stars (Li 2005). Certainly, the low frequency of disk excess found among our sample is more consistent with an older population than with million year old stars (Silverstone et al. 2006; Rieke et al. 2005; Gorlova et al. 2004).

In our survey, the WTTSs with excesses are most often found within dark clouds or adjacent to known CTTSs. V836 Tauri is on the border of Lynds 1544, Sz 82 is within 10′ of the famous emission star RU Lup, and Sz 76 lies only 20′ from the CTTS GQ Lup. Even the low-excess star RX J0432.8+1735 is located within L1551 near GG Tauri. Only RX J1603.2−3239 is a relatively isolated source. Thus, it appears that only the WTTSs that are projected onto dark clouds and CTTSs have a measureable excess. No excesses are measured for WTTSs more than 1° off-cloud. An additional source of contaminating young stars is present for the Lupus star formation region. The Sco-Cen region, with its numerous members 5–20 Myr in age, is adjacent to Lupus and potentially overlaps the regions from which our Lupus WTTSs were selected.

In order to estimate the age spread of our sample, we place our objects in the H-R diagram. We estimate the effective temperatures directly from the spectral type of the objects using the scale provided by Kenyon & Hartmann (1995). We derive the stellar luminosities by applying a bolometric correction (appropriate for each spectral type) to the *I*-band magnitudes corrected for extinction and assuming the nominal cloud distances presumed by c2d (Taurus 140 pc, Chamaeleon 178 pc, Lupus 150 pc, Oph 125 pc). An important caveat is that unresolved binary companions in our sample may produce up to a factor of 2 overestimates of stellar luminosity. The bolometric corrections were taken from Hartigan et al. (1994), and A_I was calculated using $A_I = 2.76E(R-I)$. The $(R-I)$ colors come from Kenyon & Hartmann (1995). In order to evaluate the degree of model dependence of the stellar ages we derive, we use two different evolutionary tracks to estimate stellar ages: those provided by DM97 and those presented by S00. We choose these two particular evolutionary tracks because they provide the appropriate mass and age range and are both widely used. Figure 9 shows the ages derived for our sample using both sets of evolutionary tracks and reveals a considerable age spread. The error bars for every object have been calculated by propagating into the evolutionary tracks the observational uncertainties. We adopted a $T_{\rm eff}$ uncertainty equal to one spectral type subclass and a luminosity uncertainty of 30% (dominated by the distance uncertainty for individual stars). Ages of PMS stars are very difficult to estimate due to the large observational and model uncertainties involved. However, we find that (1) even though DM97 and S00 evolutionary tracks show some systematic differences (i.e., DM97 tracks yield significantly younger ages than S00 models), the relative ages agree fairly well; and (2) the total age spread in the sample is significantly larger than the typical (observational) error bar. We also find a possible decrease in the excess frequency of WTTSs with increasing derived age, although at a low significance level. According to the DM97 models, 11% (4/37) ± 5% of the WTTSs younger than 1 Myr have a disk, while only 2% (1/46) ± 2% of the WTTSs older than 1 Myr have a disk. Similarly, the S00 models indicate that 15% (4/26) ± 7% of the WTTSs younger than 3 Myr have a disk, while only 2% (1/57) ± 2% of the older stars do. Even presuming that our stars are at the distance of the star-forming regions with which they are associated, about

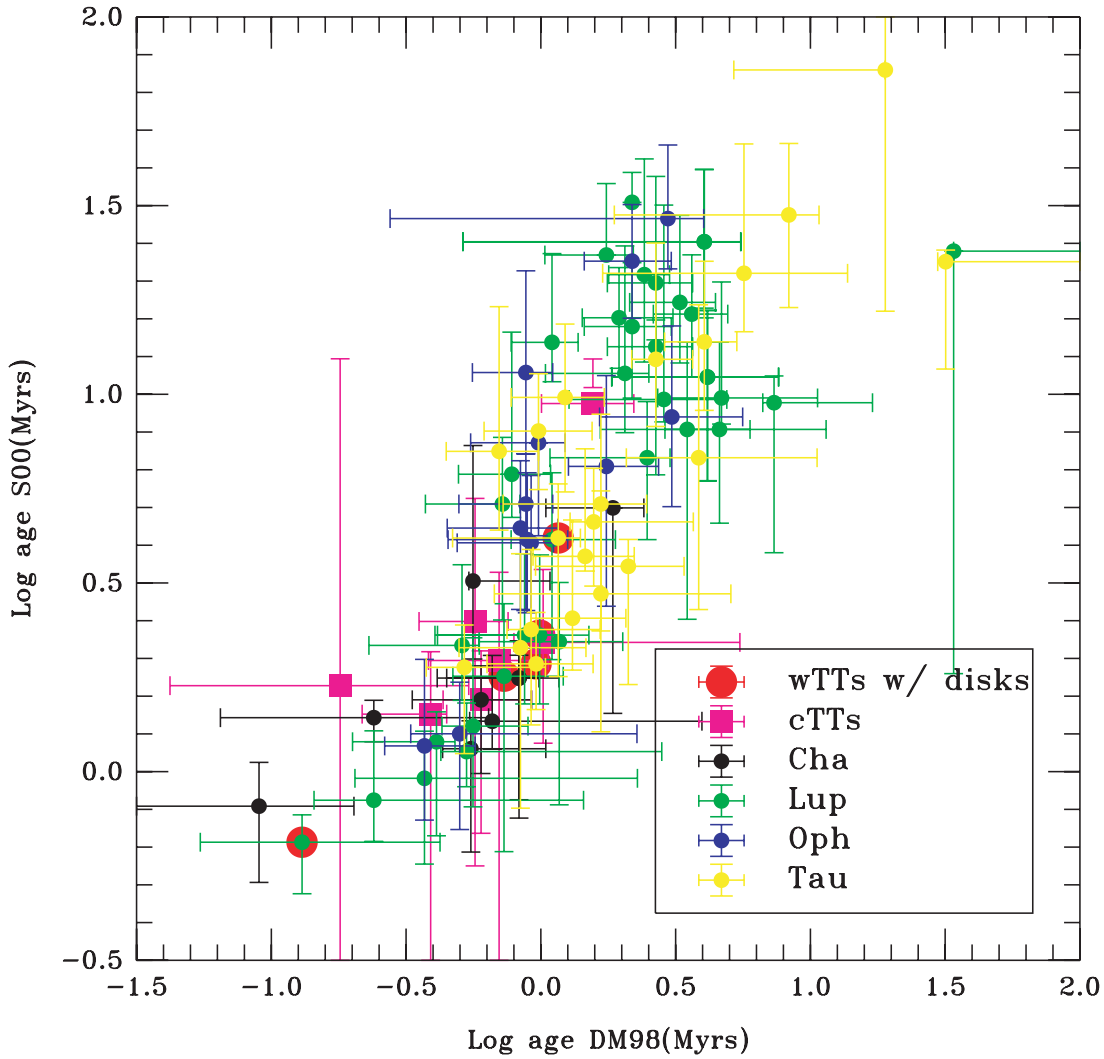

FIG. 9.— Ages of WTTSs with and without disks as derived from the model tracks of S00 and DM97. Note that the distance uncertainties to the stars dominate this plot.

one-third of the stars have properties that are consistent with an older population. The few sources with excess are among the presumably younger part of the sample, although many apparently diskless stars are also among the youngest. In the future, careful distance determinations will be required to eliminate main-sequence interlopers from the true WTTS sample.

5. CONCLUSIONS

We have detected 24 μm excess emission from only 5 of 83 weak-line T Tauri stars observed by the *Spitzer* "Cores to Disks" legacy project. The frequency for excess at $\lambda < 10$ μm is even lower (3/83); thus, two WTTSs only have excess at 24 μm. These may possess optically thin disks. The other three have SEDs indistinguishable from CTTSs and Hα EWs near the arbitrary 10 Å dividing line between CTTSs and WTTSs. According to our results and those of Hartmann et al. (2005a), solar-type PMS stars seem to predominantly be either diskless or surrounded by optically thick disks. There is no large population of optically thin disks around WTTSs. Based on these preliminary results, we conclude that both optically thick and optically thin warm disks are rare among young solar-type stars with low Hα emission. This finding suggests that some stars may pass through the Class II stage in less than 1–3 Myr. *Spitzer* observations at greater depth are required to determine whether the incidence of cold outer disks (excess at $\geq$70 μm) for WTTSs is consistent with the field. Further work is also required to determine the fraction of contaminating ZAMS foreground stars in current WTTS lists. A final caveat is that frequencies of apparently optically thin 24 μm excess among the WTTS population are low enough so that confusion with background galaxies in the 6″ *Spitzer* beam cannot be ruled out as the source of the excess for individual objects.

We acknowledge the use of C. Dullemond's cgplus publicly available disk models in Dullemond et al. (2001). We thank the Lorentz Center of the Leiden Observatory for hosting a meeting in summer 2005 at which much of this work was performed. Support for this work, which is part of the *Spitzer* Legacy Science Program, was provided by NASA through contracts 1224608, 1230782, and 1230799 issued by the Jet Propulsion Laboratory, California Institute of Technology, under NASA contract 1407. This publication makes use of data products from the Two Micron All Sky Survey, which is a joint project of the University of Massachusetts and the Infrared Processing and Analysis Center funded by NASA and the National Science Foundation. We also acknowledge use of the SIMBAD database.

REFERENCES

Adams, F. C., Lada, C. J., & Shu, F. H. 1987, ApJ, 312, 788
Alcala, J. M., Chavarria, K. C., & Terranegra, L. 1998, A&A, 330, 1017
André, P., & Montmerle, T. 1994, ApJ, 420, 837
Andrews, S. M., & Williams, J. P. 2005, ApJ, 631, 1134
Backman, D. E., & Paresce, F. 1993, in Protostars and Planets III, ed. E. Levy & J. Lunine (Tucson: Univ. Arizona Press), 1253
Beckwith, S. V. W., Sargent, A. I., Chini, R. S., & Gusten, R. 1990, AJ, 99, 924
Beichman, C., et al. 2005, ApJ, 622, 1160
Boss, A. P. 2001, ApJ, 563, 367
Bryden, G., et al. 2006, ApJ, 636, 1098
Carballo, R., Wesselius, P. R., & Whittet, D. C. B. 1992, A&A, 262, 106
Carkner, L., Feigelson, E. D., Kyoama, K., Montmerle, T., & Reid, I. N. 1996, ApJ, 464, 286
Carkner, L., Mamajek, E., Feigelson, E., Neuhaeuser, R., Wichmann, R., & Krautter, J. 1997, ApJ, 490, 735
Chen, C. H., Jura, M., Gordon, K. D., & Blaylock, M. 2005, ApJ, 623, 493
Chiang, E. I., & Goldreich, P. 1999, ApJ, 519, 279
Covino, E., Alcala, J., Allain, S., Bouvier, J., Terranegra, L., & Krautter, J. 1997, A&A, 328, 187
D'Alessio, P., Merín, B., Calvet, N., Hartmann, L., & Montesinos, B. 2005, Rev. Mex. AA, 41, 61
D'Antona, F., & Mazzatelli, I. 1997, Mem. Soc. Astron. Italiana, 68, 807 (DM97)
Ducourant, C., Teixeira, R., Périé, J. P., Lecampion, J. F., Guibert, J., & Sartori, M. J. 2005, A&A, 438, 769
Dullemond, C. P., Dominik, C., & Natta, A. 2001, ApJ, 560, 957
Duvert, G., Guilloteau, S., Ménard, F., Simon, M., & Dutrey, A. 2000, A&A, 355, 165
Evans, N. J., et al. 2003, PASP, 115, 965
Fazio, G. G., et al. 2004, ApJS, 154, 10
Franchesini, A., et al. 2005, AJ, 129, 2074
Goldreich, P., Lithwick, Y., & Sari, R. 2004a, ApJ, 614, 497
———. 2004b, ARA&A, 42, 549
Gorlova, N., et al. 2004, ApJS, 154, 448
Gras-Velázquez, À., & Ray, T. P. 2005, A&A, 443, 541
Guedel, M., Padgett, D., & Dougados, C. 2006, in Protostars and Planets V, ed. B. Reipurth, in press
Haisch, K. E., Jayawardhana, R., & Alves, J. 2005, ApJ, 627, L57
Haisch, K. E., Lada, E. A., & Lada, C. J. 2001, ApJ, 553, L153
Hanson, R. B., Klemola, A. R., Jones, B. F., & Monet, D. G. 2004, AJ, 128, 1430
Hartigan, P., Strom, K. M., & Strom, S. E. 1994, ApJ, 427, 961
Hartmann, L. 2003, ApJ, 585, 398
Hartmann, L., Megeath, S. T., Allen, L., Luhman, K., Calvet, N., D'Alessio, P., Franco-Hernandez, R., & Fazio, G. 2005a, ApJ, 629, 881
Hartmann, L., Stauffer, J. R., Kenyon, S. J., & Jones, B. F. 1991, AJ, 101, 1050
Hartmann, L., et al. 2005b, ApJ, 628, L147
Harvey, P. M., et al. 2006, ApJ, in press
Herbig, G. H., & Bell, K. R. 1988, Lick Obs. Bull., 1111, 1
Hughes, J., Hartigan, P., Krautter, J., & Keleman, J. 1994, AJ, 108, 1071
Isella, A., & Natta, A. 2005, A&A, 438, 899
Joy, A. H. 1945, ApJ, 102, 168
Kenyon, S. J., & Hartmann, L. 1987, ApJ, 323, 714
———. 1995, ApJS, 101, 117
Kohler, R., & Leinert, C. 1998, A&A, 331, 977
Krautter, J., Wichmann, R., Schmitt, J. H. M. M., Alcala, J. M., Neuhauser, R., & Terranegra, L. 1997, A&AS, 123, 329
Lada, C., Muench, A., Luhman, K., Hartmann, L., Megeath, T., Myers, P., Fazio, G., & Wood, K. 2006, AJ, 131, 1574
Li, J. Z. 2005, Ap&SS, 298, 525
Low, F., Smith, P. S., Werner, M., Chen, C., Krause, V., Jura, M., & Hines, D. C. 2005, ApJ, 631, 1170
Lyo, A. R., Lawson, W. A., Mamajek, E. E., Feigelson, E. D., Sung, E. C., & Crause, L. A. 2003, MNRAS, 338, 616
Martín, E. L., & Maguzzù, A. 1999, A&A, 342, 173
Martín, E. L., Montmerle, T., Gregorio-Hetem, J., & Casanova, S. 1998, MNRAS, 300, 733
Massarotti, A., Latham, D. W., Torres, G., Brown, R. A., & Oppenheimer, B. D. 2005, AJ, 129, 2294
Megeath, S. T., Hartmann, L., Luhman, K. L., & Fazio, G. G. 2005, ApJ, 634, L113
Mendes, L. T. S., D'Antona, F., & Mazzatelli, I. 1999, A&A, 341, 174
Meyer, M. R., et al. 2004, ApJS, 154, 422
Mundt, R., Walter, F. M., Feigelson, E. D., Finkenzeller, U., Herbig, G. H., & Odell, A. P. 1983, ApJ, 269, 229
Muzerolle, J., et al. 2004, ApJS, 154, 379
Nürnberger, D., Brandner, W., Yorke, H. W., & Zinnecker, H. 1998, A&A, 330, 549
Nürnberger, D., Chini, R., & Zinnecker, H. 1997, A&A, 324, 1036
Osterloh, M., & Beckwith, S. V. W. 1995, ApJ, 439, 288
Padgett, D., et al. 2004, ApJS, 154, 433
Padgett, D. L., Stapelfeldt, K. R., Krist, J., Watson, A., Ménard, F., & Burrows, C. 1999, BAAS, 194, 69.01
Papovich, C., et al. 2004, ApJS, 154, 70
Reach, W. T., et al. 2004, ApJS, 154, 385
Rieke, G. H., et al. 2004, ApJS, 154, 25
———. 2005, ApJ, 620, 1010
Rowan-Robinson, M., et al. 2005, AJ, 129, 1183
Sartori, M. J., Lépine, J. R. D., & Dias, W. S. 2003, A&A, 404, 913
Schwartz, R. D. 1977, ApJS, 35, 161
Sicilia-Aguilar, A., et al. 2006, ApJ, 638, 897
Siess, L., Dufour, E., & Forestini, M. 2000, A&A, 358, 593 (S00)
Silverstone, M., et al. 2006, ApJ, 639, 1138
Skrutskie, M. F., Dutkevitch, D., Strom, S. E., Edwards, S., Strom, K. M., & Shure, M. A. 1990, AJ, 99, 1187
Spite, M., Francois, P., Nissen, P. E., & Spite, F. 1996, A&A, 307, 172
Stauffer, J. R., et al. 2005, AJ, 130, 1834
Strom, K. M., Strom, S. E., Edwards, S., Cabrit, N., & Skrutskie, M. F. 1989, AJ, 97, 1451
Vinkovic, D., Ivezic, Z., Jurkick, C., & Elitzur, M. 2006, ApJ, 636, 348
Walter, F. M. 1986, ApJ, 306, 573
Webb, R. A., Zuckerman, B., Platais, I., Patience, J., White, R. J., Schwartz, M. J., & McCarthy, C. 1999, ApJ, 512, L63
Weidenschilling, S. J. 2000, Space Sci. Rev., 92, 295
Werner, M. W., et al. 2004, ApJS, 154, 1
White, R. J., Ghez, A. M., Reid, I. N., & Schultz, G. 1999, ApJ, 520, 811
White, R. J., & Hillenbrand, L. A. 2004, ApJ, 616, 998
Wichmann, R., Bouvier, J., Allain, S., & Krautter, J. 1998, A&A, 330, 521
Wichmann, R., Covino, E., Alcalá, J. M., Krautter, J., Allain, S., & Hauschildt, P. H. 1999, MNRAS, 307, 909
Wichmann, R., Krautter, J., Covino, E., Alcala, J. M., Neuhaeuser, R., & Schmitt, J. H. M. M. 1997, A&A, 320, 185
Wichmann, R., et al. 1996, A&A, 312, 439
———. 2000, A&A, 359, 181
Wolk, S. J., & Walter, F. M. 1996, AJ, 111, 2066
Young, K. E., et al. 2005, ApJ, 628, 283